Published in final edited form as:
Science. 2013 January 4; 339(6115): 70–74. doi:10.1126/science.1227622.

The Spatial and Temporal Origin of Chandelier Cells in Mouse Neocortex

Hiroki Taniguchi[*], **Jiangteng Lu**, and **Z. Josh Huang**[†]
Cold Spring Harbor Laboratory, Cold Spring Harbor, NY 11724, USA

Abstract

Diverse γ-aminobutyric acid–releasing interneurons regulate the functional organization of cortical circuits and derive from multiple embryonic sources. It remains unclear to what extent embryonic origin influences interneuron specification and cortical integration because of difficulties in tracking defined cell types. Here we followed the developmental trajectory of chandelier cells (ChCs), the most distinct interneurons that innervate the axon initial segment of pyramidal neurons and control action potential initiation. ChCs mainly derive from the ventral germinal zone of the lateral ventricle during late gestation and require the homeodomain protein Nkx2.1 for their specification. They migrate with stereotyped routes and schedule and achieve specific laminar distribution in the cortex. The developmental specification of this bona fide interneuron type likely contributes to the assembly of a cortical circuit motif.

A fundamental issue in understanding cortical circuitry concerns the origin of the identity and diversity of γ-aminobutyric acid–releasing interneurons, basic components of inhibitory circuit organization and assembly. Diverse interneurons regulate the delicate balance and dynamic operation of cortical networks (1) and are generated from the medial and caudal ganglionic eminence (MGE and CGE) of the basal ganglia and the preoptic area (2). However, there has been continued debate on what constitutes an interneuron type (3) and to what extent the phenotypic descriptions that are used to empirically distinguish cell populations reflect the intrinsic biological processes, such as their developmental specification. This is in part due to the difficulty in tracking the developmental history of any distinct interneurons, from their origin to integration into the cortical network.

Among cortical interneurons, the chandelier cell (ChC) (4) displays exceptional stereotypy and specificity: They innervate the axon initial segment (AIS), site of action potential initiation, of pyramidal neurons (PyNs) (5) and likely represent a bona fide interneuron type. A single ChC innervates hundreds of PyNs and may exert powerful control over the spiking

[†]To whom correspondence should be addressed. huangj@cshl.edu.
[*]Present address: Max Planck Florida Institute, One Max Planck Way, Jupiter, FL 33458, USA.

Supplementary Materials
www.sciencemag.org/cgi/content/full/science.1227622/DC1
Materials and Methods
Figs. S1 to S8
Tables S1 to S2
References (20, 21)
Movie S1

of a PyN ensemble; thus, together they might constitute a “basic motif” of cortical circuits. However, since their discovery nearly four decades ago, the developmental origin and cortical organization of ChCs have remained elusive.

The homeodomain protein NKX2.1 is specifically expressed by medial ganglionic eminence (MGE) progenitors (6). NKX2.1 regulates the formation of the MGE (6) and the specification of cortical interneurons (7). We found that after the MGE morphologically flattened by about embryonic day 15 (~E15), NKX2.1 expression continued at the ventral germinal zone (VGZ) of the lateral ventricle (Fig. 1, A to C), likely a remnant or extension of MGE, and persisted into the first postnatal week. Along the rostral-caudal axis of VGZ, NKX2.1$^+$ cells were restricted toward the middle-caudal region (Fig. 1, A and C); they expressed progenitor and mitotic markers (Fig. 1C and fig. S1) and incorporated 5-bromo-2′-deoxyuridine (BrdU) (8). We generated an *Nkx2.1*^{CreER} knock-in mouse (8), with inducible site-specific Cre recombinase (CreER), to achieve a genetic fate mapping of the NKX2.1$^+$ VGZ cells (Fig. 1B), focusing on late gestation and neonatal stages.

A tdTomato red fluorescent protein (RFP) reporter (9) induced by tamoxifen in E17 *Nkx2.1*^{CreER}*;Ai9* embryos labeled radial glialike progenitors along the middle-caudal regions of VGZ (Fig. 1E). VGZ-derived neurons migrated along the lateral wall of the ventricle, reaching the cortex by E18 to postnatal day 0 (P0) (Fig. 1, C, E, and J). Emerging from the dorsal-lateral side of the ventricle wall, migrating neurons split into both medial and lateral streams to populate the ventricular zone of the cortex by P1 (Fig. 1, G and J). In addition to this route, neurons generated from the middle-caudal VGZ must also migrate anteriorally, along the ventricle wall and/or within the VZ of cortex, to populate the rostral cortical areas (Fig. 1, A and D). After entering the cortex, migrating neurons first passed through the cortical plate, reaching layer1 (L1) by P2 to P3 (Fig. 1H, fig. S2, and movie S1). These cells remained and likely spread in L1 for several more days before descending back into the cortex, forming a dense band of cells at the L2-L1 border (Fig. 1, I and J). There was also a significant population of neurons reaching deep layers between P3 and P7 (Fig. 1, H to J), although their migration route and schedule are less clear.

When we assessed the identity of E17 VGZ-derived neurons after the third postnatal week, a large majority of RFP$^+$ cells in L2 turned out to be chandelier cells [91.0% in medial prefrontal cortex (mPFC), 91.8% in cingulate cortex, 71.6% in somatosensory cortex], which extend highly characteristic axon arbors with dense “cartridges” of vertically oriented strings of synaptic boutons (Fig. 2). Among the RFP$^+$ non-ChCs, some were parvalbumin$^+$ (PV$^+$) and likely fast-spiking basket cells and others were unidentified, as they were negative for somatostatin, calretinin, and vasointestinal peptide. Patch clamp recording of L2 ChCs in mPFC revealed distinct intrinsic properties compared with fast-spiking basket interneurons (fig. S3 and tables S1 and S2). Paired-recording of two nearby ChCs (within 100 μm) demonstrated weak yet extensive (14 of 16 ChC pairs, or 90%) electrical coupling. In addition, a single spike in an L2 ChC occasionally also generated di-synaptic glutamatergic inputs both to the nearby ChC and back to itself (fig. S4). These results substantiate recent studies (10, 11) and further suggest that nearby ChCs might activate each other by firing an intermediate population of PyNs, at least in cortical slices in vitro. Through electrical coupling and di-synaptic excitation, nearby ChCs might form a coherent

network. Therefore, in addition to ganglionic eminence and preoptic area, VGZ of the lateral ventricle represents a novel source of cortical interneurons and mostly generates chandelier cells. These VGZ-derived ChCs showed a striking laminar pattern, with particular enrichment in upper L2 and in L5 and L6 (Fig. 2, A and B). Our induction procedure did not label all ChCs, given the consideration that the efficiency of CreER recombination is not 100% and the fact that we observed more ChCs with two doses of tamoxifen induction (e.g., at E17 and P0); we were unable to assess the percentage of ChCs that was labeled. Nonetheless, multiple experiments showed that ChCs were significantly more abundant in the frontal cortex (cingulate and pre- and infralimbic) compared with sensory cortex (primary visual and auditory) (Fig. 2, A and C, and fig. S5).

The somata of L2 ChCs often pressed against the L2-L1 border (Fig. 2, E and F). They extended multiple dendrites to L1 and L2. Their axons exhibited the classic chandelier-like morphology, with local arbors extending a dense array of vertical strings of synaptic boutons in L2/3. Colabeling with AIS markers demonstrated that ChC terminals not only aligned to the AIS of PyNs but in fact further targeted the distal portion of AIS (Fig. 2F) (the first terminal of ChC cartridge is 10.6 ± 0.4 μm distal from the proximal end of the AIS), which accumulates the low-threshold sodium channel *Nav1.6* and is the exact site of spike initiation (12). This result unequivocally demonstrates the exquisite specificity of ChC synapses, suggested previously by vesicular GABA transporter staining of putative ChC terminals in human cortex (13). L5 ChCs extended straight apical dendrites into supragranular layers and basal dendrites within L5; their axon arbors elaborated both below and above the soma, forming dense cartridges at AIS of local PyNs (Fig. 2, A and G, and fig. S6). L6 also contained ChCs, which innervated PyNs with characteristic strings of boutons (Fig. 2H), but these cartridges appeared in multiple orientations that likely reflected the horizontal or inverted orientations of L6 PyN AISs. Given their distinct laminar location, and dendrite and axon arborization, ChCs in layers 2, 5, and 6 are likely recruited by distinct cortical and subcortical inputs and regulate different populations of PyNs. Therefore, we have identified three subgroups of ChCs, or axo-axonic cells (5), in mouse neocortex.

A widely held notion is that ChCs are a subset of PV^+ interneurons, a majority of which are fast-spiking basket cells. However we found that only a subset of ChCs tested PV^+ by immunostaining, and this fraction varied from ~50% in barrel cortex to ~15% in mPFC (Fig. 2D and fig. S7). This difference in PV levels among ChCs might reflect subtle specializations or variations in physiological states.

During the assembly of the multilayered neocortex, PyNs (14) and interneurons (15) are integrated in an “inside-out” manner, with later-born cells migrating past earlier-born populations to occupy more superficial laminae. MGE-derived interneurons that share birthdates with PyNs preferentially populate the same cortical layer (16). To examine the temporal profile of ChC production and their correlation to laminar deployment, we injected a single pulse of BrdU into pregnant *Nkx2.1*^{CreER}*;Ai9* females at successive days between E15 and P1 to label mitotic progenitors, each paired with a pulse of tamoxifen at E17 to label $NKX2.1^+$ cells (Fig. 3A). We first quantified the fraction of L2 ChCs (identified by morphology) in mPFC that were also $BrdU^+$. Although there was ChC production by E15, the peak was at E16, when MGE has morphologically disappeared and NKX2.1 expression

has appeared at VGZ (Fig. 3, B and C). ChC genesis then diminished but persisted to the end of gestation. This result significantly extends the time course of interneuron generation from NKX2.1 progenitors and suggests that ChCs may be the last cohort, generated at a time when PyN neurogenesis has largely completed. More surprisingly, we found that L5 and L6 ChCs were also $BrdU^+$ after E17 induction (Fig. 3, D and E), which indicated that they were generated long after L5 and L6 PyNs, and as late as L2 ChCs. Therefore, the laminar deployment of ChCs does not follow the inside-out sequence, further distinguishing them from MGE-derived interneurons.

NKX2.1 expression during late gestation also included the preoptic area and striatum (6). To prove VGZ as the source of ChCs, we labeled $NKX2.1^+$ cells at E16, then transplanted the RFP^+ VGZ progenitors to the somatosensory cortex of P3 wild-type hosts (Fig. 4, A to B). After 3 weeks, these exogenous progenitors not only differentiated into neurons that spread to the medial frontal areas and settled into appropriate laminar (e.g., L2 and L5) but further matured into quintessential ChCs (Fig. 4, C and D). These results indicate that $NKX2.1^+$ progenitors in the late embryonic VGZ are the main source of ChCs. They further demonstrate that the identity of a ChC is determined by its spatial and temporal origin (i.e., lineage and birth time) and, once specified, a cell autonomous program can unfold in ectopic locations, even without proper migration, to direct differentiation.

To examine the role of NKX2.1 in ChC specification, we deleted *Nkx2.1* in VGZ progenitors using a conditional strategy (fig. S8) and transplanted NKX2.1-deficient VGZ cells to the somatosensory cortex of wild-type pups (Fig. 4E). These $Nkx2.1^{KO}$ progenitors gave rise to neurons that accumulated in L2 and L5 after 3 weeks (Fig. 4G), a laminar pattern that resembled those of endogenous ChCs. However, $Nkx2.1^{KO}$ lineage cells did not differentiate into ChCs, as indicated by the lack of L1 dendrites and almost absence of cartridgelike axon terminals (Fig. 4, F and G). Together with previous studies (6, 7), our results suggest that NKX2.1 may regulate the appropriate temporal competence of progenitors, which likely undergo sequential changes with cell division. They further indicate that NKX2.1 expression in VGZ progenitors is necessary to complete the specification of a distinct and probably the last cohort in this lineage—the ChCs.

A recent study demonstrated that progenitors below the ventral wall of the lateral ventricle (i.e., VGZ) of human infants give rise to a medial migratory stream destined to the ventral-medial PFC (17). Despite species differences in the developmental timing of corticogenesis, this and our studies raise the possibility that the $NKX2.1^+$ progenitors in VGZ and their extended neurogenesis might have evolved, since rodents, to enrich and diversify cortical interneurons, including ChCs.

Studies in numerous systems (18) have demonstrated that the specification of neuronal identities early in development exerts strong influences in their subsequent positioning, connectivity, and function, but to what extent this principle applies to the assembly of cortical circuits has been unclear. Here we discovered that young chandelier cells, once specified through their lineage and birth time in the VGZ, migrate with stereotyped route and achieve distinct laminar patterns before innervating a subdomain of PyN AIS. Therefore, interneurons with a distinct identity are likely endowed with cell-intrinsic

programs that contribute to their subsequent integration into destined cortical networks. Deficiencies in ChCs have been implicated in brain disorders, including schizophrenia (19). Genetic targeting of ChCs establishes an entry point that integrates studies of fate specification, laminar deployment, connectivity, and network dynamics in the context of cortical circuit assembly and function. This may provide a probe to circuit pathogenesis in models of neuropsychiatric disorders.

Supplementary Material

Refer to Web version on PubMed Central for supplementary material.

Acknowledgments

We would like to thank G. Miyoshi for technical advice of fate-mapping experiments and helpful discussion. Support by NIH R01 MH094705. H.T. is a PRESTO (Precursory Research for Embryonic Science and Technology) investigator supported by Japan Science and Technology Agency (JST) and was supported by a Brain and Behavior Research Foundation (NARSAD) Postdoctoral Fellowship. J.L. is in part supported a Patterson Foundation Postdoctoral Fellowship. Z.J.H. is supported by the Simons Foundation and a NARSAD Distinguished Investigator award.

References and Notes

1. Markram H, et al. Interneurons of the neocortical inhibitory system. Nat Rev Neurosci. 2004; 5:793.10.1038/nrn1519 [PubMed: 15378039]
2. Gelman DM, Marín O. Generation of interneuron diversity in the mouse cerebral cortex. Eur J Neurosci. 2010; 31:2136.10.1111/j.1460-9568.2010.07267.x [PubMed: 20529125]
3. Ascoli GA, et al. Petilla terminology: Nomenclature of features of GABAergic interneurons of the cerebral cortex. Nat Rev Neurosci. 2008; 9:557.10.1038/nrn2402 [PubMed: 18568015]
4. Szentágothai J, Arbib MA. Conceptual models of neural organization. Neurosci Res Program Bull. 1974; 12:305. [PubMed: 4437759]
5. Somogyi P. A specific ‘axo-axonal’ interneuron in the visual cortex of the rat. Brain Res. 1977; 136:345.10.1016/0006-8993(77)90808-3 [PubMed: 922488]
6. Sussel L, Marin O, Kimura S, Rubenstein JL. Loss of Nkx2.1 homeobox gene function results in a ventral to dorsal molecular respecification within the basal telencephalon: Evidence for a transformation of the pallidum into the striatum. Development. 1999; 126:3359. [PubMed: 10393115]
7. Butt SJ, et al. The requirement of Nkx2-1 in the temporal specification of cortical interneuron subtypes. Neuron. 2008; 59:722.10.1016/j.neuron.2008.07.031 [PubMed: 18786356]
8. Taniguchi H, et al. A resource of Cre driver lines for genetic targeting of GABAergic neurons in cerebral cortex. Neuron. 2011; 71:995.10.1016/j.neuron.2011.07.026 [PubMed: 21943598]
9. Madisen L, et al. A robust and high-throughput Cre reporting and characterization system for the whole mouse brain. Nat Neurosci. 2010; 13:133.10.1038/nn.2467 [PubMed: 20023653]
10. Szabadics J, et al. Excitatory effect of GABAergic axo-axonic cells in cortical microcircuits. Science. 2006; 311:233.10.1126/science.1121325 [PubMed: 16410524]
11. Woodruff A, Xu Q, Anderson SA, Yuste R. Depolarizing effect of neocortical chandelier neurons. Front Neural Circuits. 2009; 3:15.10.3389/neuro.04.015.2009 [PubMed: 19876404]
12. Hu W, et al. Distinct contributions of Na(v)1.6 and Na(v)1.2 in action potential initiation and backpropagation. Nat Neurosci. 2009; 12:996.10.1038/nn.2359 [PubMed: 19633666]
13. Inda MC, DeFelipe J, Muñoz A. Voltage-gated ion channels in the axon initial segment of human cortical pyramidal cells and their relationship with chandelier cells. Proc Natl Acad Sci USA. 2006; 103:2920.10.1073/pnas.0511197103 [PubMed: 16473933]
14. Angevine JB Jr, Sidman RL. Autoradiographic study of cell migration during histogenesis of cerebral cortex in the mouse. Nature. 1961; 192:766.10.1038/192766b0 [PubMed: 17533671]

15. Fairén A, Cobas A, Fonseca M. Times of generation of glutamic acid decarboxylase immunoreactive neurons in mouse somatosensory cortex. J Comp Neurol. 1986; 251:67.10.1002/cne.902510105 [PubMed: 3760259]

16. Miller MW. Cogeneration of retrogradely labeled corticocortical projection and GABA-immunoreactive local circuit neurons in cerebral cortex. Brain Res. 1985; 355:187. [PubMed: 3910166]

17. Sanai N, et al. Corridors of migrating neurons in the human brain and their decline during infancy. Nature. 2011; 478:382.10.1038/nature10487 [PubMed: 21964341]

18. Jessell TM. Neuronal specification in the spinal cord: Inductive signals and transcriptional codes. Nat Rev Genet. 2000; 1:20.10.1038/35049541 [PubMed: 11262869]

19. Lewis DA. The chandelier neuron in schizophrenia. Dev Neurobiol. 2011; 71:118.10.1002/dneu.20825 [PubMed: 21154915]

20. Kusakabe T, et al. Thyroid-specific enhancer-binding protein/NKX2.1 is required for the maintenance of ordered architecture and function of the differentiated thyroid. Mol Endocrinol. 2006; 20:1796.10.1210/me.2005-0327 [PubMed: 16601074]

21. Southwell DG, Froemke RC, Alvarez-Buylla A, Stryker MP, Gandhi SP. Cortical plasticity induced by inhibitory neuron transplantation. Science. 2010; 327:1145.10.1126/science.1183962 [PubMed: 20185728]

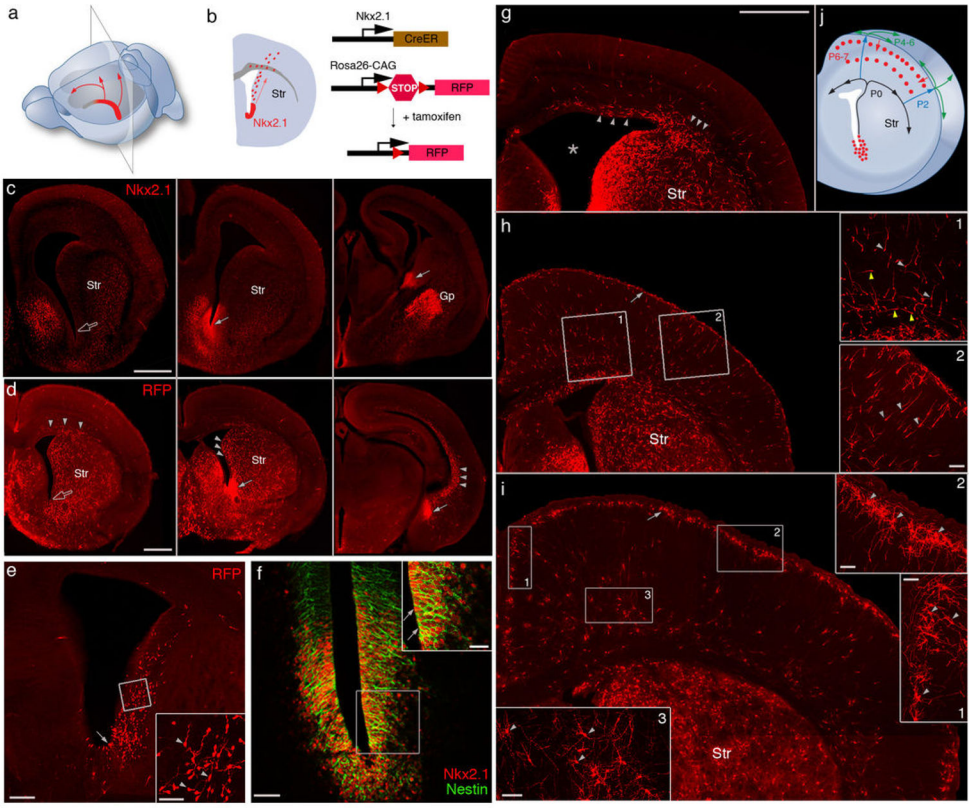

Fig. 1.

Nkx2.1^{+} progenitors in the embryonic VGZ are a novel source of cortical interneurons. (**A**) NKX2.1 expression (red) in middle-caudal regions of the late embryonic VGZ. Arrows indicate the migration of VGZ-derived cells toward the dorsal and rostral cortex. (**B**) A coronal section from a region indicated in (A). Red dots represent VGZ-derived cells migrating toward the cortex. Genetic fate mapping strategy is depicted to the right. In an *Nkx2.1^{CreER};Ai9* mouse, Cre-mediated recombination is induced by tamoxifen and activates RFP expression. Str, striatum. (**C**) Immunofluorescence showing NKX2.1 protein (arrows) in the middle-to-caudal region (middle and right panels) but not rostral region (open arrow in left panel) of E17 VGZ. (**D**) *Nkx2.1^{CreER};Ai9* mice induced at E17 and examined at E18. RFP-labeled progenitors were abundant in the middle-caudal regions (solid arrows) but not rostral region (open arrow) of VGZ. RFP^{+} migrating cells (arrowheads) were found not only in midcaudal sections but also in the rostral section. (**E**) Coronal section of an E18 brain induced by low-dose tamoxifen. More sparse VGZ progenitors (arrow) and postmitotic cells (arrowheads in inset) are labeled, giving a clearer view of the migratory stream along the lateral wall of the ventricle. (**F**) Colocalization (arrow) of NKX2.1 and Nestin in VGZ progenitors shown by double immunostaining. (**G**) Coronal section of a P0 brain induced at E17. Migrating cells emerge from the dorso-lateral wall of the ventricle (star) and split into lateral and medial stream (arrowheads) within the cortical subventricular zone. (**H**) Coronal section of a P2 brain induced at E17. Migrating cells, each with a characteristic leading process (arrowheads in insets) pass through cortical plate into L1 (arrow). (Insets) Tangentially migrating cells in the subventricular and intermediate zone (yellow

arrowheads, H1) and radially migrating cells in the cortical plate (light gray arrowheads, H2). (**I**) Coronal section of a P7 brain induced at E17. RFP^+ cells descend from L1 into the cortex and settle at the L1/L2 border (arrow), forming dense clusters, and start to differentiate (arrowheads in I1 and I2). Deep-layer RFP^+ cells (arrowheads in I3) also settle and show sign of differentiation by this stage but their migration route is unclear. (**J**) Diagram depicting the migration route and schedule of VGZ-derived cortical cells. Scale bars: 500 μm in (C), (D), and (G to I); 200 μm in (E); 50 μm in (F) and insets of (E), (H), and (I); and 25 μm in inset of (F).

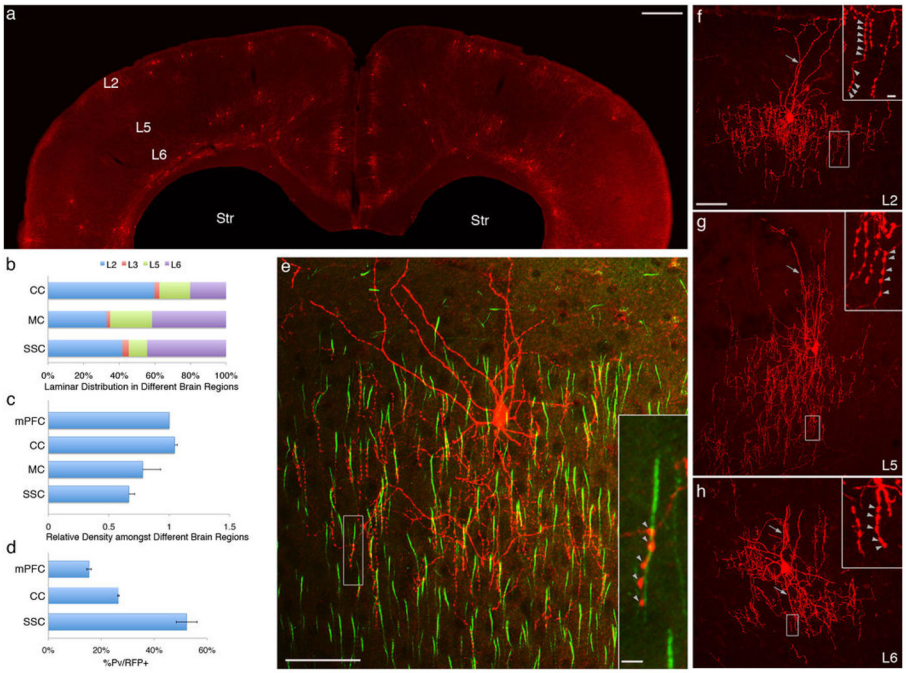

Fig. 2.

Areal and laminar distribution of ChCs in neocortex. (**A**) Coronal section showing the overall distribution of RFP$^+$ neurons at P28 after E17 induction of an *Nkx2.1^{CreER};Ai9* mouse. (**B**) Laminar distribution of RFP$^+$ cells in cingulate (CC), motor (MC) and somatosensory (SSC) cortices. (**C**) L2 RFP$^+$ cells are more abundant in medial frontal cortices (mPFC, CC) compared with sensory cortices (SSC); ~70% and 90% of RFP$^+$ cells are ChCs in SSC and mPFC, respectively. (**D**) C-expression of PV in L2 RFP$^+$ cells varies greatly across cortical areas. (**E**) Colabeling of pyramidal cell AIS [phosphorylated inhibitor of nuclear factor κB (IκB), green] and an L2 ChC. Terminal cartridges align with AISs and target the distal portion of AISs (arrowheads in inset). (**F**) An L2 ChC with characteristic chandelier-like axon arbor and terminal cartridges bearing strings of synaptic boutons (arrowheads in inset). Note the prominent L1 dendrites (arrow). (**G**) An L5 ChC with characteristic chandelier-like axon arbor and terminal cartridges (arrowheads in inset). Note the relatively straight apical dendrites (arrow). (**H**) An L6 ChC with dense local axon arbor and terminal cartridges (arrowheads in inset); its dendrites (arrows) extend above and below the soma. Scale bars: 500 μm in (A), 50 μm in (E) and (F–H), and 5 μm in insets of (E) and (F–H).

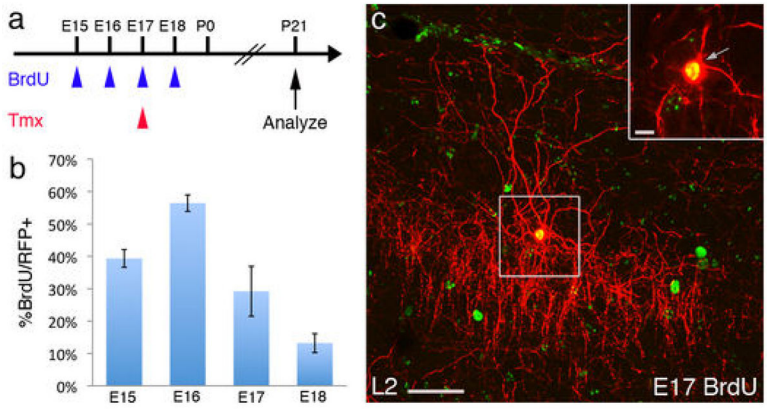

Fig. 3.

Temporal profile of ChC generation in the NKX2.1 lineage. (**A**) Scheme of ChC birth dating. In an *Nkx2.1*^{CreER}*;Ai9* mouse, NKX2.1 lineage cells are labeled by tamoxifen (Tmx) induction at E17 (red arrowhead), paired with a single BrdU injection at the indicated date (blue arrowheads). Mice were analyzed for colocalization after P21. (**B**) The temporal profile of L2 ChC generation in the cingulate cortex, with a peak at E16. (**C**) A BrdU-labeled L2 ChC. (**D** and **E**) L5 and L6 ChCs are also born in the late embryonic stage. A ChC in L5 (D) and L6 (E) labeled by BrdU at E17, tamoxifen-induced at E17, and analyzed at P28. Insets are single confocal sections. Scale bars: 50 μm in (C) to (E) and 10 μm in insets.

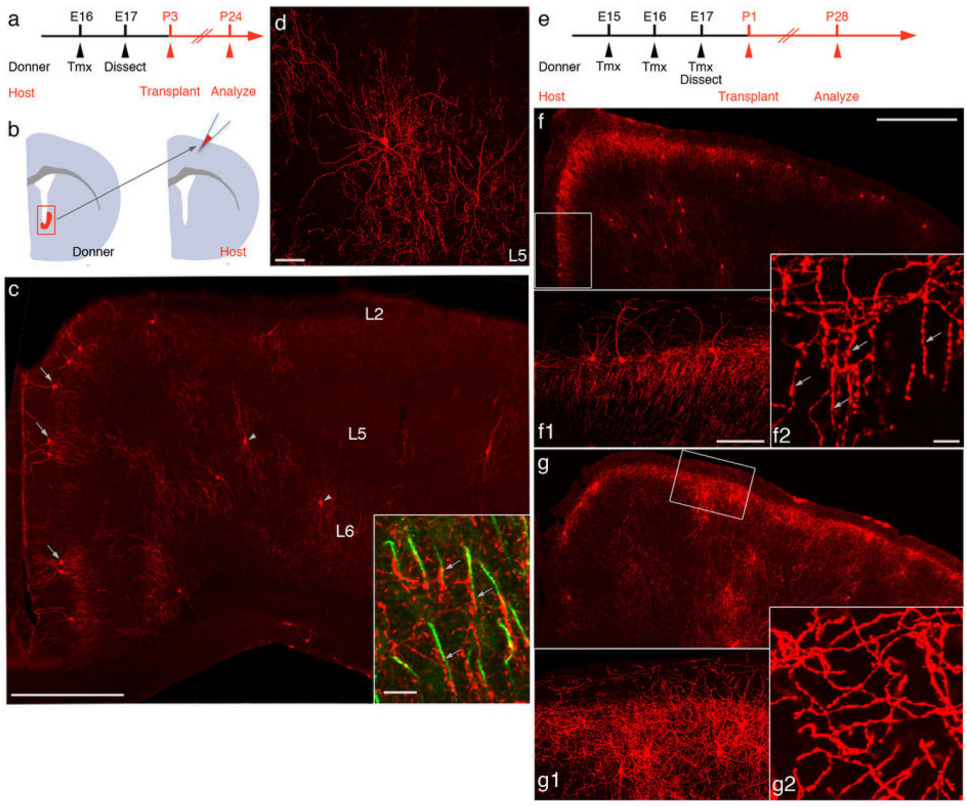

Fig. 4.

NKX2.1 in VGZ progenitors is necessary for the specification of ChCs. (**A**) Scheme of transplantation experiment. *Nkx2.1*^{CreER}*;Ai9* donors are induced at E16 with tamoxifen (Tmx); RFP-labeled cells from VGZ are dissected at E17 and transplanted to the somatosensory cortex of P3 wild-type host pups and analyzed at P24. (**B**) The transplantation of RFP^{+} VGZ cells to a wild-type brain. (**C**) Coronal section of a P24 host cortex in which ChCs differentiated from transplanted RFP^{+} VGZ cells. L2 (arrows) and L5 ChCs (arrowheads) are readily identified. The laminar distribution of transplanted ChCs closely resembles that of endogenous ChCs, and L2 ChCs extend characteristic L1 dendrites and local axon arbors. Inset, transplanted ChC axon terminals (arrows) innervate PyNs at AIS (phosphorylated IκB, green) (**D**) High-magnification view of a transplanted L5 ChC with characteristic dendritic and axon morphology. (**E**) Scheme of transplantation from *Nkx2.1*$^{CreER/fix}$(*Nkx2.1*^{KO})*;Ai9* embryos. Animals are induced three times from E15 to E17, and RFP^{+} VGZ cells are transplanted into P1 wild-type pups. In the same set of experiments, *Nkx2.1*$^{CreER/+}$(*Nkx2.1*$^{+/-}$)*;Ai9* mice were used as controls. (**F**) Coronal section of a P28 host brain transplanted with *Nkx2.1*$^{+/-}$ VGZ cells. ChCs accumulate in L2-L1 border, as well as in L5. Higher-magnification view of a boxed region shows dense vertical-oriented axon terminals (F1), with characteristic strings of boutons (F2). (**G**) Neurons derived from *Nkx2.1*^{KO} VGZ cells accumulate in L2 and L5, but fail to differentiate into ChCs. Higher-magnification view of the boxed region shows a lack of L1 dendrites and vertical oriented

axon terminals (G1), with almost a complete absence of terminal cartridges, (G2). Scale bars: 500 μm in (C), (F), (G); 100 μm in (F1) and (G1); 10 μm in (F2) and (G2).